Atmospheric pressure induced atomic diffusion into solid crystal

J. K. Bal and S. Hazra*

Surface Physics Division, Saha Institute of Nuclear Physics, 1/AF Bidhannagar, Kolkata 700064, India

Gaussian-shape diffused nanolayer, formed due to atomic diffusion of gold into silicon crystal, shows wave-front-like movement with time when the system is in ambient condition, while it remains almost static as long as it is in ultrahigh vacuum condition. This is clear evidence of simple atmospheric pressure induced diffusion of atomic gold into the silicon crystal and provides an interesting concept of inherent pressure inside a crystal structure. The atmospheric pressure at the surface and its gradual decreasing nature from the surface to inside crystal acts as driving and retarding forces, respectively, which can be used to control the formation and movement of the diffused layer in nanolevel. Such diffusion also depends on the crystal structure and freeness of the diffusing atoms. The latter increases as the thickness and/or coverage of the gold layer decreases.

PACS number(s): 66.30.Pa, 68.35.Fx, 68.37.−d, 61.05.cm

I. INTRODUCTION

The Au/Si interface, which is probably the most studied metal-semiconductor contact,[1–13] is a model system for investigating the Schottky-barrier formation as well as the nature of p-d hybridization process.[6,7] A variety of experimental methods has been applied to obtain complementary information on electronic and structural properties of Au/Si interface.[3–5] It is found that Au reacts with Si surface to form interfacial layer even at room temperature and ultrahigh vacuum (UHV) condition,[2] in contrary to Ag which forms a rather abrupt interface with Si. Although the thickness where the interfacial layer formed has some controversy,[1–12] following junction structure from the Si substrate is well accepted at least for the thicker-layer case: a diffuse and alloyed zone (about 2 nm thick); an intermediate region where only Au is detected and a thin (about 1–2 ML) superficial phase on top of the Au region.[4,6] It is known that most of the semiconductors readily reacting with the metals are classified as covalent semiconductors with fairly large bond energy. Consequently, the above interfacial reaction may hardly occur without the presence of such an effect of metal as to induce instability in covalent bonding (or cohesive character) of the semiconductor adjacent to the metal. The possible cause of the instability (say in Si) is the ability of metal (say Au) to screen Coulomb interaction due to its mobile free electrons.[4]

The interfacial layer formed at the Au/Si interface under ambient conditions is somewhat different.[13] Formation of broad diffused nanolayer of different widths and compositions have been observed using nondestructive x-ray reflectivity (XRR) technique,[14] where the surface stability due to the surface pretreatment and/or passivation conditions provide such control. The question is: do we understand the process responsible for that observed enhanced diffusion behavior? Although, there are lot of processes, namely, the high reactivity of Au with Si as discussed before, the Au deposition condition (e.g., deposition energy), effect of Fermi level and/or concentration of interstitials and vacancies in surface region (e.g., due to native Si oxidation), etc., which can be accountable for the formation of initial very thin diffused

layer or enhancement of the atomic diffusion[15–17] near Si surface but cannot explain completely the observed diffusion behavior and hence needs proper understanding. Here, with that aim we have performed further experiments on Au-Si system and observed that Gaussian-shape diffused nanolayer, which is formed, shows shock wavelike[18] diffusion behavior under ambient condition, while it remains almost static under UHV condition. We have shown that this kind of anomalous diffusion behavior actually helps us in identifying the process, namely, atmospheric pressure induced atomic diffusion into solid crystal.

II. EXPERIMENT

For the present work, Au thin film of different thickness have been deposited on H-passivated Si(001) substrates using magnetron sputtering units (PLS 500, Pfeiffer or T4065, KVS). Prior to deposition, as obtained Si(001) substrate was cut into pieces (each of size about 10×10 mm^2) and were sonicated by trichloroethelene (for about 10 min) and methyl alcohol (for about 10 min) separately to remove organic contaminations. Hydrofluoric acid (HF, 10%) was then used to remove the native oxide layer, which also help to form relatively stable H-passivated Si(001) surface. These substrates were loaded into the sputtering chambers for Au deposition, where the power and the argon pressure were maintained either at 25 W and 3.5×10^{-3} mbar, respectively (in PLS 500), or at 9 W and 2.7×10^{-2} mbar, respectively (in T4065). Samples are designated as $S1$ and $S2$, prepared together initially have thickness about 4 nm. For checking the reproducibility, samples designated as $S3$ and $S4$ of same thickness have been prepared again. To see the effect of thickness, samples designated as $S5$ and $S6$ of thickness about 9 and 13 nm, respectively, have been prepared (which also have high coverage compared to samples $S1-S4$). Lastly, samples designated as $S7$ and $S8$ of thickness about 4 nm have been prepared for keeping those samples at nitrogen atmosphere.

XRR measurements of Au-Si samples were carried out using a versatile x-ray diffractometer (VXRD) setup as a function of time to see the interfacial evolution due to diffu-

sion. VXRD consists of a diffractometer (D8 Discover, Bruker AXS) with Cu (sealed tube) source followed by Göbel mirror to select and enhance Cu $K\alpha$ radiation (λ =1.54 Å). The diffractometer has a two-circle goniometer $[\theta(\omega)-2\theta]$ with quarter-circle Eulerian cradle as sample stage. The latter has two circular (χ and ϕ) and three translational (X, Y, and Z) motions. Scattered beam was detected using NaI scintillation (point) detector. Data were taken in the specular condition, i.e., the incident angle (θ) is equal to the exit angle (θ) and different tight slits are placed before and after the sample. Under such condition, a nonvanishing wave-vector component, q_z, is given by $(4\pi/\lambda)\sin\theta$ with resolution 0.0014 Å^{-1}. Analysis of XRR data has been carried out using Parratt's formalism.[19] For the analysis, each film has been divided into a number of layers including roughness at each interface.[20] Analysis of XRR data essentially provides an electron-density profile (EDP), i.e., in-plane (x-y) average electron density (ρ) as a function of depth (z) in high resolution. From the electron density, it is then possible to estimate the mass density (ρ_m, as ρ_m is proportional to ρ for single material[21]) and the diffuse amount and its position. To see the evolution of EDP, XRR data for one set of samples were collected as a function of time after keeping that set at ambient conditions; while for other set of samples, XRR data have been collected just before and after the samples were in UHV (pressure $<10^{-9}$ mbar) condition. It is necessary to mention that some time is always required to attend the UHV condition from ambient condition or *visa-a-visa* during transfer into the chamber or when taking out of it. Also to separate out the effect of oxygen and atmospheric pressure on diffusion, XRR measurements have been carried out for another set of samples after keeping those samples for different duration in nitrogen environment having similar atmospheric pressure. Slightly enhanced diffusion in nitrogen environment has been observed compared to ambient conditions.

The topography of the Au films at different stages of interdiffusion at ambient conditions were mapped through atomic force microscopy (beam-deflection AFM, Omicron NanoTechnology) in different portions of the samples and in different length scales (50–1000 nm) to get statistically meaningful information. AFM images were collected in non-contact mode[22] and in UHV conditions to get high-resolution stable and clean images. WSXM software[23] has been used for the processing and analysis of AFM images.

To verify the existence of the interdiffused layer as predicted from XRR measurements, cross-sectional scanning electron microscopy (SEM) (Quanta 200 FEG) have been performed by breaking some of the samples after prolonged interdiffusion. Even top Au layer has been removed by simple scratching, among some of those samples before breaking. Typical SEM images of a sample, with or without top Au layer, are shown in Figs. 1(a) and 1(b). Also XRR measurements have been carried out, with similar samples having prolonged interdiffusion, just after removing the top Au layer using aqua regia and also after removing the subsequent SiO$_2$/Si layer by HF etching. Typical XRR data along with the analyzed curves are shown in Fig. 1(c). It can be noted that SEM images and the EDP [shown in the inset of Fig. 1(c)] confirm the presence of diffused nanolayer.
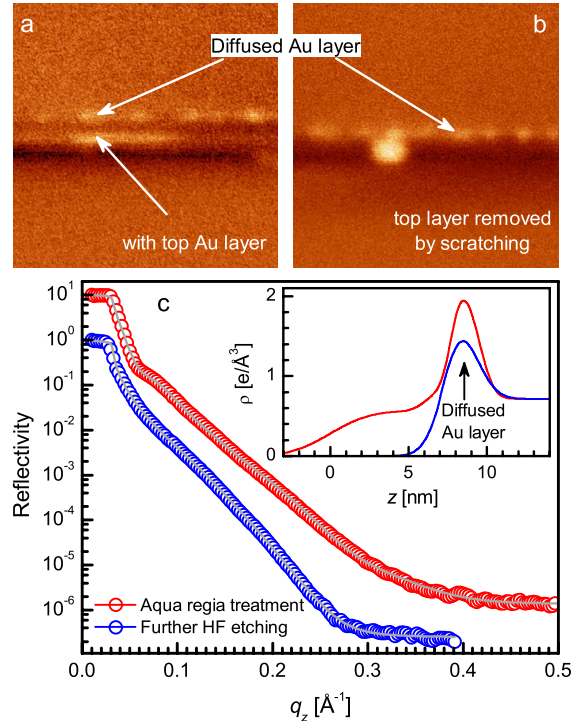

FIG. 1. (Color online) Cross-sectional SEM images of one of the diffusion samples (a) with or (b) without top Au layer. Presence of diffused layer is clearly evident. (c) XRR data (symbols) and analyzed curves (solid lines) just after removing the top Au layer using aqua regia and also after removing the subsequent SiO$_2$/Si layer by HF etching of one of the diffused samples. Inset: corresponding EDPs, which also confirm the presence of diffused layer.

III. RESULTS AND DISCUSSION

The evolution of XRR data for the Au-Si system under ambient and UHV conditions are shown in Fig. 2(a). Corresponding EDP are shown in Fig. 2(b). Formation of broad diffused nanolayer is evident from the EDP. Such layer shows movement with time when it is in ambient condition, while it remains almost static when it is in UHV condition. The evolution of topography due to strong interdiffusion has been observed from AFM images. Typical time-evolution AFM images are shown in Figs. 3(a) and 3(b). Corresponding height-histogram and coverage as a function of height are shown in Fig. 3(c). Variation in coverage with time obtained from AFM images is consistent with the change in the corresponding EDP shown in the inset of Fig. 3(c).

In order to understand the diffusion behavior, diffusion length (L), obtained from the EDP, is plotted in Fig. 4(a) as a function of time. It is clear from Fig. 4(a) that L changes with time monotonically when it is under ambient condition and deviates from that behavior when it is under UHV condition. It is also clear that if we ignore the time during which the sample is under UHV condition, then considering modified time, the value of L almost falls into that ambient condition curve. The monotonic variation in L, however, does not follow $t^{1/2}$ dependence, which is clearly evident from Fig. 4(b). Also the diffusivity (D) plotted against L in the inset of Fig. 4(b) shows that D deviates from constant value. In fact, D decreases with length.
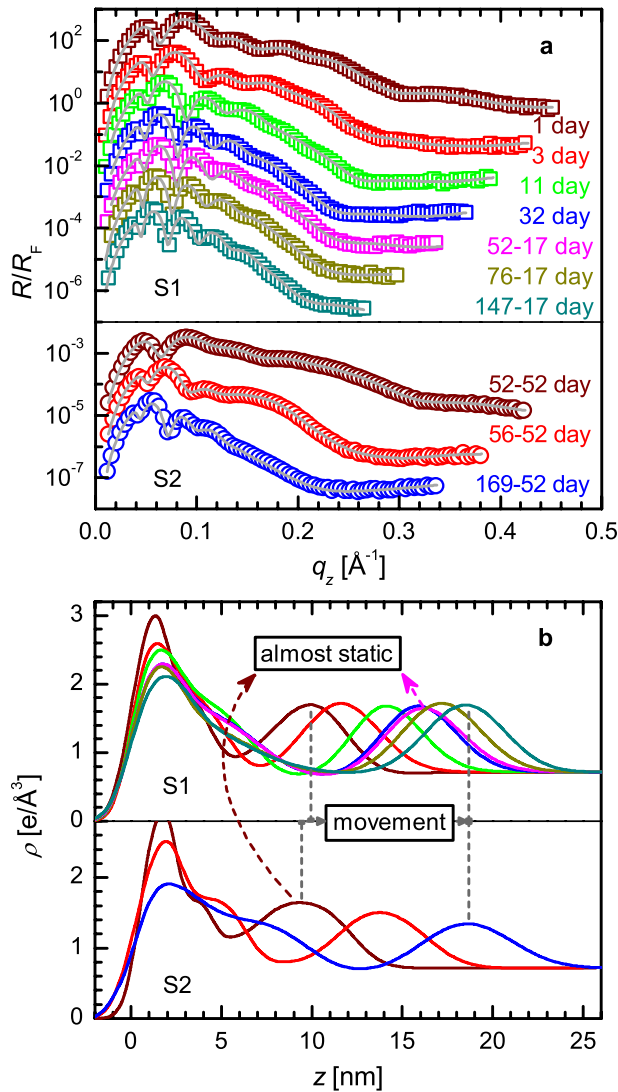
FIG. 2. (Color online) (a) Time-evolution (top to bottom) normalized XRR data (in symbols) and analyzed curves (in solid lines) for two similar samples (S1 and S2). Both samples were mostly in ambient conditions (namely, in atmospheric pressure), except, sample S1 was in UHV for about 17 days (from day 35 to day 52), while sample S2 was in UHV for about 52 days (from day 0 to day 52). Curves are shifted vertically for clarity. Kiessig fringes in the curves move toward left with time in presence of atmospheric pressure, indicative of increase in thickness. (b) Corresponding time-evolution (left to right) EDPs for two samples. Movement of the diffused layer inside silicon with time is evident in presence of atmospheric pressure.

The diffusion process, in general, can be characterized by a barrier with activation energy E_a, where E_a is the energy required to jump from one site to the next site. The probability of an atom jumping to another site is given by the product of two terms: the first term is the frequency, ν_0, with which the atom collides with the barrier and the second term is the probability that the atom will surmount the barrier during a collision [$\exp(-E_a/kT)$, where k is Boltzmann's constant and T is the temperature]. Accordingly, the diffusivity can be written as[24]

FIG. 3. (Color online) Typical AFM images (of scan size 800 $\times 800$ nm^2) showing topography (a) almost after deposition and (b) after diffusion at atmospheric pressure for about 35 days. (c) Corresponding height-histogram and coverage as a function of height. Coverage at a given height (indicated by a dashed line, for example) decreases with time due to diffusion of gold into silicon, consistent with the EDP (and corresponding dashed line) shown in the inset.

$$D = \frac{4\nu_0 d^2}{6} e^{-E_a/kT} = D_0 e^{-E_a/kT}. \tag{1}$$

If the value of D is sufficient then it is expected to observe diffusion and considering random symmetric diffusion (i.e., D is independent of both time and space), the diffused amount should follow Fick's law. However, strong deviation from the Fickian $t^{1/2}$ dependence[25] is observed in the Au-Si system.[13] The deviation has been well understood considering the growth of blocking oxide layer at the interface with time, assuming D is sufficiently large to observe the diffusion. The growth of oxide layer at the interface, which takes place due to the presence of oxygen at ambient condition, blocks the diffusion. Accordingly, it was expected that if one can prevent or slow down the oxide growth at the interface (namely, by placing the system at UHV condition) then diffusion should enhance. However, with surprise we observed quite contrary, namely, diffusion and/or movement of diffused layer when the system is in ambient condition, while almost no diffusion or stagnation of diffused layer, when it is in UHV condition (Figs. 2 and 4). These simple observations suggest that the assumption, D is sufficiently large to observe the diffusion, is not correct and open up fundamental question regarding diffusion in such system in particular and atomic diffusion in solid system[26] in general.

In silicon, gold atoms can either move around or displace silicon atoms [Fig. 5(a)]. The first one is the interstitial diffusion, which requires relatively low activation energy (E_i), while the latter one is the substitutional diffusion, which requires relatively high activation energy (E_s). So, the question
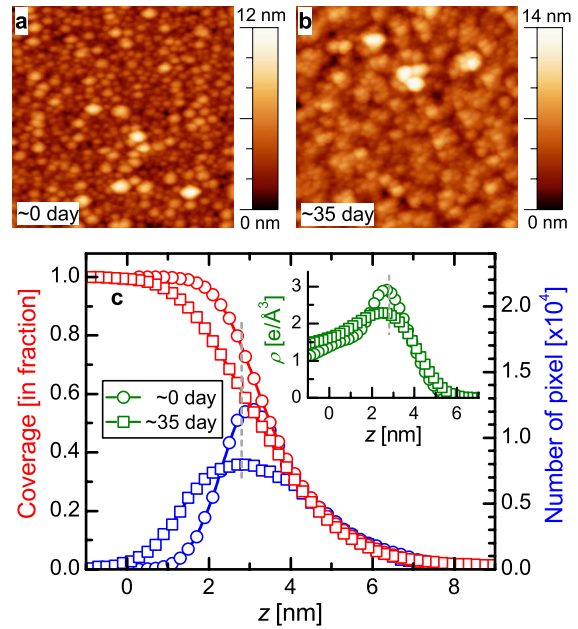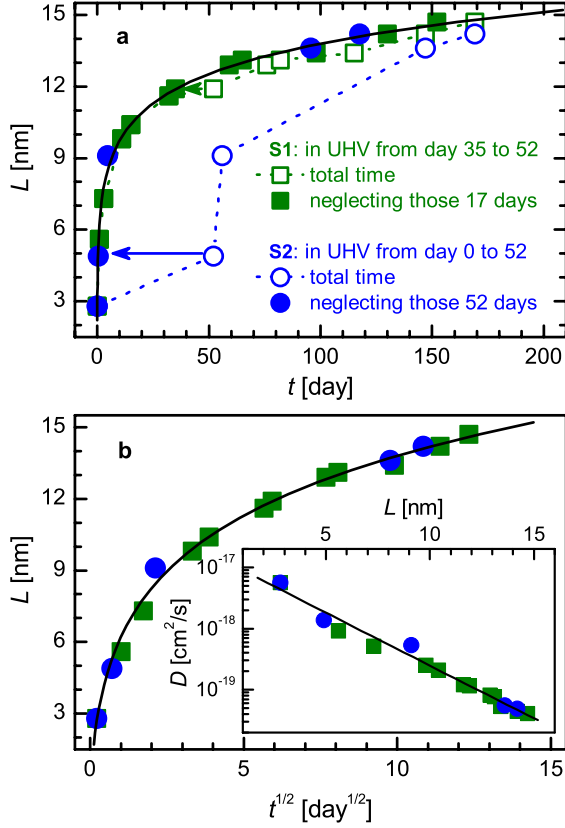
FIG. 4. (Color online) (a) Diffusion length (L) as a function of time for two samples ($S1$ and $S2$). L (in symbols) has been derived from the EDP. The total time (partly in atmospheric pressure and partly in UHV) as well as the time only in atmospheric pressure (neglecting the time that was inside UHV condition) were used for the plotting to get the clear idea that there is no change in L when the sample is in UHV and the clear evidence of atmospheric pressure induced atomic diffusion into solid. (b) Diffusion length as a function of square root of time (that it was in atmospheric pressure) to show the deviation from normal $t^{1/2}$ dependence (which should be a straight line). Inset: diffusivity as a function of length. All solid lines represent analyzed curves considering the effective diffusivity, arising mainly due to atmospheric pressure and its exponential dependence on length.

is that even if we consider interstitial diffusion, does the room temperature is sufficient to supply required activation energy ($E_a = E_i \approx 0.5$ eV)? If not, how does diffusion take place? In the following we will argue that this can be understood considering the strong role of atmospheric pressure in diffusion. The results suggest that when the system is in ambient condition, the atmospheric pressure is helping to overcome the diffusion barrier,[27] while when the system is in UHV condition no such driving force is there. The blocking of diffusion due to the growth of oxide layer comes into picture only when diffusion can take place. Also, this clearly indicates that the pressure inside a crystal (P_c), particularly in silicon is intermediate between atmospheric pressure to UHV. So in general, if we consider P_0 is the outside pressure that acts on the surface of the film and $P_s (= c_P P_0)$ is the pressure that acts on the crystal surface, where c_P is a fraction that depends on the thickness and the effective density
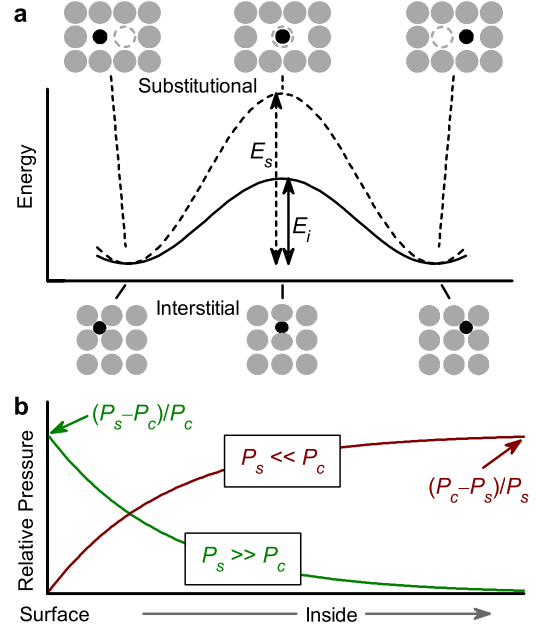

FIG. 5. (Color online) Schematic of diffusion and pressure gradient in solid crystal. (a) Two types of diffusion having different barrier energy. The activation energy required for the interstitial diffusion (E_i) is quite small compared to that for the substitutional diffusion (E_s). Still, the room temperature (kT) is not sufficient to supply that small activation energy (E_i), while the atmospheric pressure, creating a pressure gradient, can supply that energy. (b) Relative pressure variation from surface to inside bulk for two extreme cases. Depending upon the value of the surface pressure (P_s) relative to the inherent-pressure (P_c), interdiffused nanolayer not only form but also moves inside (for $P_s \gg P_c$) or remains static (for $P_s \approx P_c$) or even diffuses outward (for $P_s \ll P_c$) with time.

of the film, then $P_s - P_c$ is the effective pressure difference and $(P_s - P_c)/P_c$ is the normalized term that acts on the surface, which should decay gradually inside the crystal [for $P_s \gg P_c$ in Fig. 5(b)]. Considering exponential decay (along z direction) with decay length λ_c, which can be considered as a characteristic length scale of that crystal structure, the effective diffusivity (D_{eff}) can be written as

$$D_{\text{eff}} = D\left(1 + \frac{P_s - P_c}{P_c}\right)e^{-z/L_c}, \qquad (2)$$

where $L_c (= c_L \lambda_c)$ is the effective decay length and c_L is a fraction that decides the initial freeness of the diffusing atoms.[28] $c_L \approx 1$ indicates $L_c \approx \lambda_c$, which means the diffusing atoms are almost free, while deviation from 1 indicates $L_c < \lambda_c$, which means the decay is fast and the diffusing atoms are not so free. The second term within the brackets in Eq. (2) arising entirely from the effect of pressure, in absence of which, the effective diffusivity becomes normal diffusivity. At room temperature, the value of normal diffusivity is very small; so to observe appreciable diffusion, the second term must be very large compared to the first one. Considering effective diffusivity, the diffusion length can be expressed as

$$L = \sqrt{4D_{\text{eff}}t}. \qquad (3)$$

Expression (3) is obtained from Fick's second law of diffusion, which can also be obtained from Einstein-Smoluchowski equation, considering Brownian motion as a fluctuation phenomenon.[25] The diffusivity and the diffusion length in Fig. 4 have been analyzed using Eqs. (2) and (3). The analyzed curves (solid lines in Fig. 4) agree well with the experimental data. It is necessary to mention that for the present analysis, not all the parameters are independently very sensitive, as it mainly provides the value of L_c and combined value of $D \times (P_s - P_c)/P_c$, which are 2.5 nm and 1.3×10^{-17} cm^2/s, respectively. Also the analysis only suggests that $D \approx 10^{-21}$ cm^2/s, which implies $(P_s - P_c)/P_c \geq 10^4$ or $P_c \leq 10^{-4} \times c_P P_0$. In our present experiment, P_0 is the atmospheric pressure that acts on the gold surface. So the value of P_c is less by more than four orders of magnitude compared to the atmospheric pressure. This means, for the present system, we get definite value of L_c only, while for other parameter, such as P_c, we get value within some range.

It is now imperative to discuss more about the two major parameters, namely, P_c, the inherent pressure inside a solid crystal structure, and λ_c, the characteristic length scale. Although, the value of P_c for a particular crystalline material should be unique, the problem is to determine that value. It is very clear from Eqs. (2) and (3) that if we perform similar experiments for different value of P_0, which are lower than that of the atmospheric pressure, then the value of P_0 will come when there will be no diffusion or no change in diffusion length at all. From that value of P_0 there is a chance to predict the value of P_c more definitely. However, the problem may be that no detectable or measurable diffusion is there for a range of outside pressure, then that will restrict the prediction of P_c beyond certain range. Nonetheless, *in situ* experiments under precise pressure-controlled environments, after growing gold thin films on clean silicon surfaces, need to be carried out for getting best possible value. At the same time, estimation of P_c from theoretical point of view is required.

Unlike normal diffusion, which depends on concentration gradient and enhanced due to increase in temperature; the concept of P_c suggests that depending upon the relative pressure difference or the direction of pressure gradient [Fig. 5(b)], one cannot only able to form the interdiffused nanolayer but also able to move that layer inside or keep that layer static or even diffuse that layer outward with time. This observation is also completely new in comparison to the effect of pressure (mainly high pressure) on diffusion, which has been studied for quite long time.[29–33] The change in diffusion on those studies has been analyzed in terms of change in the effective free volume in the crystal structure. That means, due to the application of the pressure, the crystal structure as a whole compressed or decompressed, and accordingly diffusion decreased or increased,[29–33] which is not the case here. It is well known that the out diffusion of Si is enhanced in oxygen environment, which appear at the top of Au layer.[4,6] This, however, cannot explain the shock-wave-like diffusion behavior observed here. It is likely that due to the diffusion of Au into Si some of the Si atoms are displaced
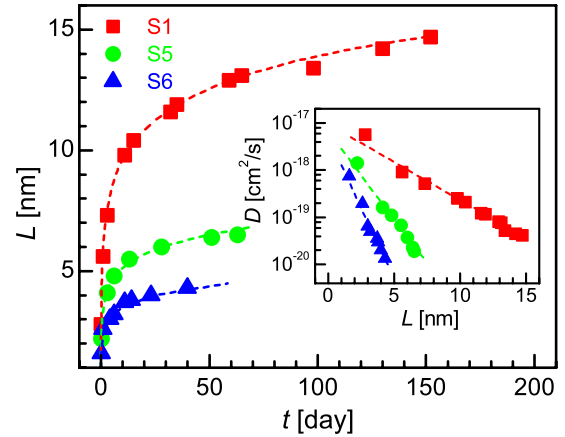

FIG. 6. (Color online) Time-evolution diffusion length and length-dependent diffusivity (in the inset) for three samples ($S1$, $S5$, and $S6$) having different film thickness (d) and/or film coverage (C) such that $d_{S1} < d_{S5} < d_{S6}$ and/or $C_{S1} < C_{S5} < C_{S6}$. All dashed lines represent analyzed curves considering the effective diffusivity, where c_P and c_L are different for three samples. Preliminary analysis of the data clearly suggests that the value of c_P and c_L decreases as the thickness and/or the coverage of the film increases.

outwards (compared to diffused layer) to release the extra stress. That displacement, if any, is enhanced not due to oxygen environment, rather due to pressure, which we have verified keeping samples in nitrogen environment of same pressure (where slightly more diffusion has been observed). It is necessary to mention that there are also other possible effects or mechanisms, namely, effect of Fermi level, effect of concentration of interstitials and vacancies in surface region (e.g., due to native Si oxidation), influence of contamination with gas atoms, and atomic collisions (energy transfer from gas atoms), etc. which can explain slight enhancement of atomic diffusion near Si surface[6,15–17] but cannot explain such pushing and stopping of the diffused layer inside Si. Coming to the parameter λ_c, it is clear from the analysis that we can only get the value of L_c and that $L_c \to \lambda_c$ when $c_L \to 1$. Although, it is difficult to know when c_L becomes 1, it is evident from the preliminary data (Fig. 6) that as the thickness and/or the coverage of the film decreases the value of c_L (also c_P) increases, i.e., the freeness of atoms increases, which is consistent with the earlier observation that the melting temperature of metal nanoparticles decreases.[34] Further experiments are require to understand the actual relationship of c_L and c_P with the thickness and/or the coverage of the film, which then can be utilized to estimate the value of λ_c.

IV. CONCLUSIONS

Present work shows clear signature of atmospheric pressure induced atomic diffusion into solid crystal and provides unique concept of inherent pressure inside a crystal structure. It also provides a characteristic length scale, which is a measure of quantitative extent of pressure gradient, from the surface to the bulk of that solid crystal. The atomic diffusion observed here is more like a fluid flow, where relative pressure acts as a regulating valve, which not only controls the

speed but also controls the direction of the flow. Apart from the pressure-gradient, such diffusion depends on the crystal structure and freeness of the diffusing atoms. Preliminary analysis suggests that the freeness of the diffusing atoms increases with decreasing thickness and/or coverage of gold layer. Further studies in this direction are necessary. Also, the diffused nanolayer formed here expected to have interesting electronic structure and transport properties. Once we have the complete control on that nanolayer in terms of concentration or composition, width or thickness, and position then it will be worth studying its interesting structure and properties.

ACKNOWLEDGMENTS

---

*satyajit.hazra@saha.ac.in

[1] C. B. Collins, R. O. Carlson, and C. J. Gallagher, Phys. Rev. **105**, 1168 (1957).

[2] L. Braicovich, C. M. Garner, P. R. Skeath, C. Y. Su, P. W. Chye, I. Lindau, and W. E. Spicer, Phys. Rev. B **20**, 5131 (1979).

[3] G. Le Lay, Surf. Sci. **132**, 169 (1983).

[4] A. Hiraki, Surf. Sci. Rep. **3**, 357 (1983).

[5] S. L. Molodtsov, C. Laubschat, G. Kaindl, A. M. Shikin, and V. K. Adamchuk, Phys. Rev. B **44**, 8850 (1991).

[6] A. Cros and P. Muret, Mater. Sci. Rep. **8**, 271 (1992).

[7] Z. Ma and L. H. Allen, Phys. Rev. B **48**, 15484 (1993).

[8] J.-J. Yeh, J. Hwang, K. Bertness, D. J. Friedman, R. Cao, and I. Lindau, Phys. Rev. Lett. **70**, 3768 (1993).

[9] K. Pedersen and P. Morgen, J. Phys.: Condens. Matter **9**, 9497 (1997).

[10] C. Grupp and A. Taleb-Ibrahimi, Phys. Rev. B **57**, 6258 (1998).

[11] J. H. Kim, G. Yang, S. Yang, and A. H. Weiss, Surf. Sci. **475**, 37 (2001).

[12] Y. Haruyama, K. Kanda, and S. Matsui, Radiat. Phys. Chem. **75**, 1943 (2006).

[13] J. K. Bal and S. Hazra, Phys. Rev. B **75**, 205411 (2007).

[14] *X-ray and Neutron Reflectivity: Principles and Applications*, edited by J. Daillant and A. Gibaud (Springer, Paris, 1999).

[15] Hans-J. Gossmann, C. S. Rafferty, H. S. Luftman, F. C. Unterwald, T. Boone, and J. M. Poate, Appl. Phys. Lett. **63**, 639 (1993).

[16] Z. H. Jafri and W. P. Gillin, J. Appl. Phys. **81**, 2179 (1997).

[17] S. C. Jain, W. Schoenmaker, R. Lindsay, P. A. Stolk, S. Decoutere, M. Willander, and H. E. Maes, J. Appl. Phys. **91**, 8919 (2002).

[18] A. N. Bekrenev, J. Phys. Chem. Solids **63**, 1627 (2002).

[19] L. G. Parratt, Phys. Rev. **95**, 359 (1954).

[20] S. Kundu, S. Hazra, S. Banerjee, M. K. Sanyal, S. K. Mandal, S. Chaudhuri, and A. K. Pal, J. Phys. D **31**, L73 (1998).

[21] S. Hazra, S. Chakraborty, and P. T. Lai, Appl. Phys. Lett. **85**, 5580 (2004).

[22] *Noncontact Atomic Force Microscopy*, edited by S. Morita, R. Wiesendanger, and E. Meyer (Springer, Heidelberg, 2002).

[23] I. Horcas, R. Fernandez, J. M. Gomez-Rodriguez, J. Colchero, J. Gomez-Herrero, and A. M. Baro, Rev. Sci. Instrum. **78**, 013705 (2007).

[24] See S. W. Jones, Diffusion in Silicon at www.icknowledge.com

[25] A. Fick, Philos. Mag. **10**, 30 (1855); J. Renn, Ann. Phys. **14**, 23 (2005); J. Philibert, Diffus. Fundam. **4**, 6.1 (2006).

[26] A. F. W. Willoughby, Rep. Prog. Phys. **41**, 1665 (1978).

[27] M. J. Aziz, S. Circone, and C. B. Agee, Nature (London) **390**, 596 (1997).

[28] R. B. Stinchcombe and F. D. A. Aarão Reis, Phys. Rev. B **77**, 035406 (2008).

[29] H. B. Vanfleet, D. L. Decker, and H. R. Curtin, Phys. Rev. B **5**, 4849 (1972).

[30] P. M. Fahey, P. B. Griffin, and J. D. Plummer, Rev. Mod. Phys. **61**, 289 (1989).

[31] O. Sugino and A. Oshiyama, Phys. Rev. B **46**, 12335 (1992).

[32] M. J. Aziz, Y. Zhao, Hans-J. Gossmann, S. Mitha, S. P. Smith, and D. Schiferl, Phys. Rev. B **73**, 054101 (2006).

[33] N. E. B. Cowern, Phys. Rev. Lett. **99**, 155903 (2007).

[34] Ph. Buffat and J.-P. Bore, Phys. Rev. A **13**, 2287 (1976).